FOUR-BAND POLARIZATION-INSENSITIVE METAMATERIAL ABSORBER BASED ON FLOWER-SHAPED STRUCTURES

Donghao Zheng, Yongzhi Cheng, Dongfang Cheng, Yan Nie, and Rongzhou Gong[*]

School of Optical and Electronic Information, Huazhong University of Science and Technology, Wuhan 430074, P. R. China

Abstract—In this paper, a four-band metamaterial absorber (MA) based on flower-shaped structure is proposed. The design, simulation, fabrication, and measurement of the absorbers working in four bands are presented. Simulation results show that the MA has four distinctive absorption peaks at frequencies 6.69 GHz, 7.48 GHz, 8.67 GHz, and 9.91 GHz with the absorptivity of 0.96, 0.99, 0.99 and 0.98, respectively. Experiment results matches well with the simulation. Both experiment and simulation results exhibit that the MA are polarization-insensitive for TE wave and TM wave. The flower-shaped structure is also suitable for designing of a four-band THz and even higher frequency MM absorber, which would be a promising candidate as absorbing elements in scientific and technical applications.

1. INTRODUCTION

Metamaterials (MMs) have gained plenty of attention during the past few years for its exotic properties, such as perfect lens [1], negative refraction [2], filters [3] and cloaks [4, 5], which can be seldom achieved by traditional materials. As an artificial medium, the permittivity and permeability of the MMs can be tuned by changing geometric dimension and shape [6]. Multi-band operation properties of MMs also can be realized by multiple-frequency resonators design [7, 8]. Generally, more or less power losses could be existence when electromagnetic (EM) waves impinge on MMs, many applications would be desirable to maximize this losses, such as the absorber. In 2008, Landy et al. [9] first presented a perfect MM absorber (MA) in

a narrow-band which can absorb all the incident EM waves by tuning the magnetic and electrical resonances. This MA maybe found some potential applications, such as thermal imaging, thermal bolometer, wavelength selective radiation, stealth technology, and so on.

To achieve perfect absorption, the designed MA usually consists of three or more layers sub-wavelength coupling structures of the electric resonator combined metal wire or sheet layer. The absorption of MAs can be defined as $A(\omega) = 1 - R(\omega) - T(\omega)$, where $A(\omega)$, $R(\omega)$, and $T(\omega)$ are the absorption, reflection, and transmission as functions of frequency ω respectively. From microwave to optical frequency, lots of MAs were proposed and investigated widely [10–17]. However, most of the MAs work only for one particular polarization or narrow-band. Then, many efforts were paid to make the MA achieve polarization-insensitive and wideband absorption to dual-band/multi-band/broadband [18–22]. However, multi-band especially four narrowband polarization insensitive MAs are seldom reported.

In this paper, we propose a four band polarization-insensitive MA based on flower-shaped structures. Simulation results show that the proposed MA has four distinctive absorption bands whose peaks are over 96%. Both simulation and experiment results exhibit that the MA is polarization-insensitive, which is potential to be used in devices such as bolometer and detection of explosives.

2. DESIGN, SIMULATION AND EXPERIMENT

The designed four-band MA was inspired by the narrow-band perfect absorber structures in Ref. [23] which were composed of flower-shaped structure sandwiched with dielectric substrate and continuous film. The unit cell of designed MA structure is displayed in Fig. 1(a). The designed MA consists of two metallic layers separated by a dielectric spacer, each of the metallic layers is copper with 30 μm in thickness and frequency independent conductivity $\sigma = 5.8 \times 10^7$ S/m. To achieve four band perfect absorptions, four flower-shaped structures with different geometrical parameters are positioned on a co-planar in a unit cell. As shown in Fig. 1(b), the each flower-shaped structure has geometry of a symmetrical four-petal flower, which is the intersections of two circles with the same area, where r is the radius. The dielectric layer is modeled as FR-4 with a permittivity of 3.55 and a loss tangent of 0.025. The optimized geometry dimension parameters of the unit cell are as follows: $t = 1.14$ mm, $p = 20$ mm, $r_1 = 4.5$ mm, $r_2 = 4$ mm, $r_3 = 3.5$ mm, $r_4 = 3$ mm.

The absorption could be calculated by using the equation $A(\omega) = 1 - R(\omega) = 1 - |S_{11}|^2$ in our design due to without transmis-
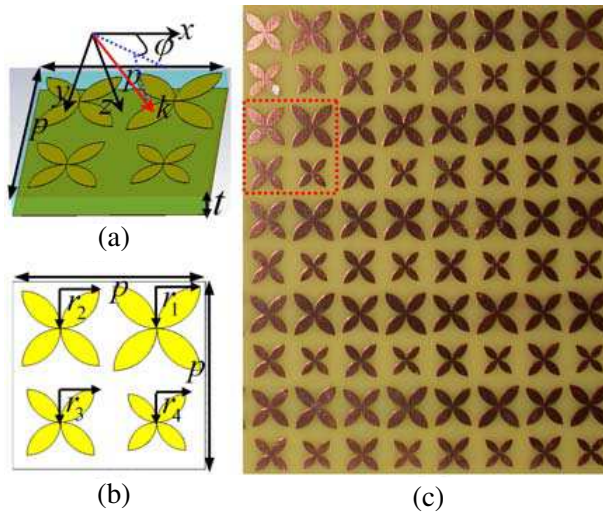
Figure 1. (a) Perspective view of the unit cell of the proposed MA, (b) front-view of the MA based on flower-shaped structures, (c) photograph of fabricated MA sample.

sion. A full wave EM simulation was performed to get the reflection parameter S_{11} based on the standard finite-difference time domain (FDTD) method. The periodic boundary conditions were applied to the x and y directions and the absorbing boundary conditions were applied to the z direction. To demonstrate the microwave absorption, the designed structures were fabricated into a 20×20 unit cell sample ($200\,\mathrm{mm} \times 200\,\mathrm{mm} \times 1.2\,\mathrm{mm}$) by the conventional printed circuit board (PCB) process with the same structural parameters as the simulation model, and the portion photography of the fabricated MA sample is shown in Fig. 1(c). Agilent PNA-X N5244A vector network analyzer connected to the two standard gain broadband linearly polarized horn antennae that produced microwaves in the range of 5–12 GHz were employed to measure the reflection of MA in an EM anechoic chamber. We can rotate the antenna polarization from $0°$ to $80°$ in $10°$ steps to verify the polarization-insensitive feature of the proposed absorber.

3. RESULTS AND ANALYSES

The simulation and experiment results are shown in Fig. 2. The simulation results exhibit that there are four narrow bands across the entire frequency range. For simulation results, there are four absorption peaks at frequencies at 6.69 GHz, 7.48 GHz, 8.67 GHz, and
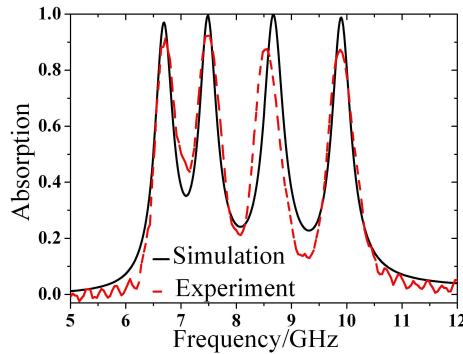
Figure 2. The simulation results (black line) and experiment results (red line) of the multi-band MA based on flower-shaped structures.

9.91 GHz with absorptivity of 0.96, 0.99, 0.99 and 0.98, respectively. It indicates that the impedance of proposed MA can be tuned to approximate match to the free space in our interested frequency range. The full width at half-maximum (FWHM) of each absorption peak is 0.46 GHz, 0.51 GHz, 0.52 GHz and 0.44 GHz, respectively. For the experiment results, which matches reasonably well with simulation results across the whole frequency range and there exist slight deviations in resonant peaks. These discrepancies are mainly due to the following two reasons: Firstly, there exist the tolerances in the fabrication and the imperfection in measurements. Secondly, it could exist the excessive smoothing in the experimental data processes.

To better understand the physical mechanism of the four bands MA, we study the power loss density distribution of the four resonances, as shown in Fig. 3. According to the previous study [23], the frequency of the flower-shaped structure MA peak can be easily controlled by adjusting the petal size without affecting the absorption. On the other hand, the MA peak frequency is linear inverse with the square root of the radius of the petals (r). Thus, the resonant frequency (f_0) of the absorption is primarily determined by radius of the petals ($f_0 \sim 1/\sqrt{r}$). As shown in Fig. 3, the four resonance peaks are corresponding to four different geometric parameters petals, and the power loss densities distributions with the four different resonant frequencies are centered on the edge of the four different petals, respectively. For four flower-shaped structures in a unit cell, four distinct located resonances are observed at 6.69 GHz, 7.48 GHz, 8.67 GHz, and 9.91 GHz as shown in the Figs. 3(a)–(d). It is also found that the power loss accumulates at the space neighboring of the petals at resonances, where the energy is significantly reinforced
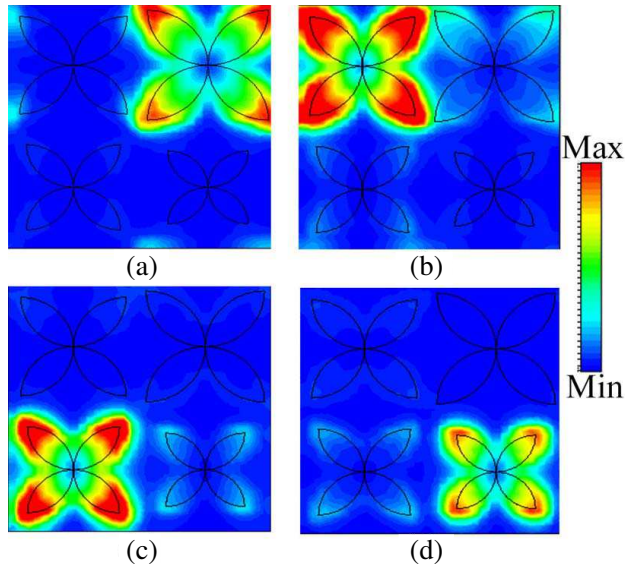
Figure 3. Distributions of the power loss density at (a) 6.69 GHz, (b) 7.48 GHz, (c) 8.67 GHz, and (d) 9.91 GHz.

and subsequently converted into thermal energy leading to strong absorption [23]. The power loss density distribution further indicates the near perfect absorptions of the four bands MA is mainly due to the local EM coupling resonance mechanism.

The absorptions of the proposed MA for different polarization angles with TE and TM modes ranging from 0° to 80° are also calculated and measured, as shown in Fig. 4. For the TE case and TM case of the simulation, the peak absorption remains greater than 95% and changes very little. While for the TE case and TM case of the experiment, the absorption peaks at resonance are about 85%, smaller than the simulation results. However, the absorptions almost keep the same for different polarization angles. The measurement environment difference and fabrication imperfection contribute to the discrepancies between simulation results and experiment ones. Both the simulated and experimental results indicate that the MA is four bands and polarization-insensitive.

In fact, the four-band perfect absorptivity can be realized at THz, infrared frequencies and even optical frequencies if the dimensions of the flower-shaped structure are reduced to micro-, nano- and even lower scale. For a typical example, we can give a design for four-band perfect absorptivity in THz region. Similar to the design of He et al. [12],
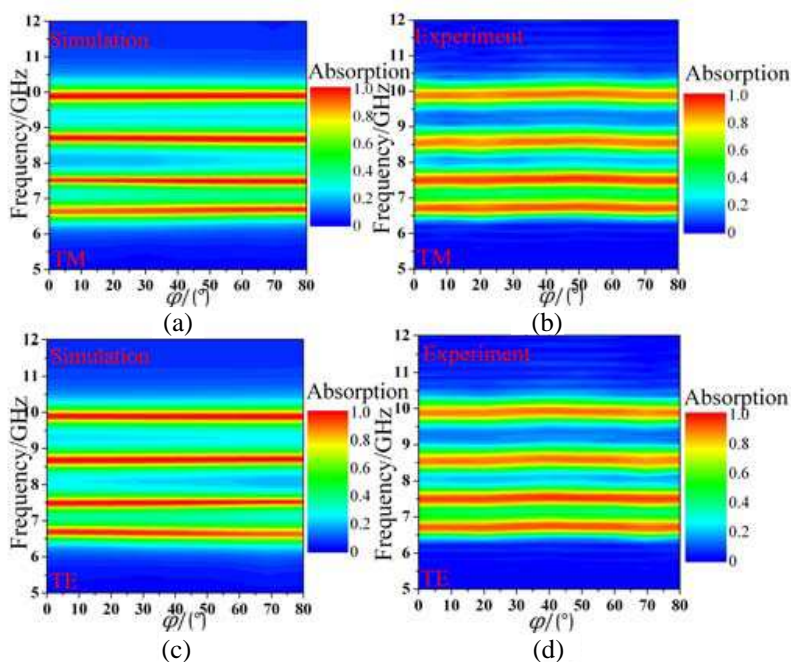
Figure 4. Absorption under different polarization angles for TM waves of (a) simulation and (b) experiment; and for TE waves of (c) simulation and (d) experiment.
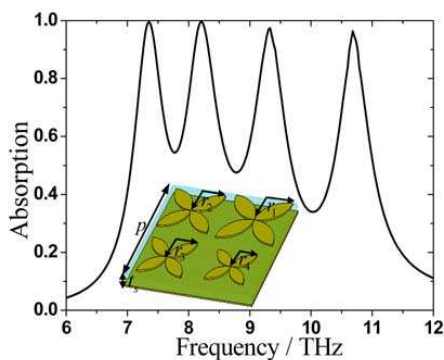
Figure 5. The simulated absorption curve of the THz four-band mm absorber; the inset shows the single unit cell.

the polyimide (lossy) with a frequency-independent permittivity of $\varepsilon = 2.88 - i0.144$ as a dielectric spacer, and two metallic layers were modeled as lossy gold film with an electric conductivity 4.09×10^7 S/m

and thickness of 0.2 μm. The single unit cell is shown in the inset of Fig. 5, and the optimal geometric parameters of the single unit cell are as follows in micrometers: $t_s = 1.3$, $p = 20$, $r_1 = 4.5$ mm, $r_2 = 4$, $r_3 = 3.5$, $r_4 = 3$. The simulation absorption is presented in Fig. 5, one can see that the absorptivity is up to 0.996, 0.997, 0.973 and 0.964 at 7.35 THz, 8.21 THz, 9.33 THz and 10.68 THz, respectively. Therefore, the flower-shaped is suitable for designing a four-band perfect THz MM absorber as well.

4. CONCLUSION

In summary, the absorption properties of a four-band MA based on flower structure are studied. The simulation results show the four absorption peaks can reach over 96%, which matches reasonably well with the experiments. The near perfect absorptions of the four-band MA is mainly due to the local EM resonance mechanism by simulating the power loss density distribution. Furthermore, both simulations and experiments exhibit that the absorptions of the deigned MA are nearly unchanged for different polarization angles with TE and TM modes. Moreover, the four-band perfect absorptivity can be realized at THz region when the dimensions of the flower-shaped structure are reduced to micro scale. Such a design can have some potential applications in thermal detectors, THz imaging and stealth.

REFERENCES

1. Pendry, J. B., "Negative refraction makes a perfect lens," *Phys. Rev. Lett.*, Vol. 85, 3966–3969, 2000.

2. Shelby, R. A., D. R. Smith, and S. Schultz, "Experimental verification of a negative index of refraction," *Science*, Vol. 292, 77–79, 2001.

3. Butt, H., Q. Dai, T. D. Wilkinson, and G. A. J. Amaratunga, "Photonic crystals & metamaterial filters based on 2D arrays of silicon nanopillars," *Progress In Electromagnetics Research,* Vol. 113, 179–194, 2011.

4. Pendry, J. B., D. Schurig, and D. R. Smith, "Controlling electromagnetic fields," *Science,* Vol. 312, 1780, 2006.

5. Schurig, D., J. J. Mock, B. J. Justice, S. A. Cummer, J. B. Pendry, A. F. Starr, and D. R. Smith, "Metamaterial electromagnetic clock at microwave frequencies," *Science*, Vol. 314, 977–980, 2006.

6. Maxim, V. G., I. V. Shadrivov, and Y. S. Kivshar, "Enhanced parametric processes in binary metamaterials," *Appl. Phys. Lett.*, Vol. 88, 071912, 2006.

7. Chen, H., L. Ran, J. Huangfu, X. Zhang, K. Chen, T. M. Grzegorczyk, and J. A. Kong, "Metamaterial exhibiting left-handed properties over multiple frequency bands," *J. Appl. Phys.*, Vol. 96, 5338, 2004.

8. Sydoruk, O., O. Zhuromskyy, and E. Shamonina, "Phonon-like dispersion curves of magnetoinductive waves," *Appl. Phys. Lett.*, Vol. 87, 072501, 2005.

9. Landy, N. I., S. Sajuyigbe, J. J. Mock, D. R. Smith, and W. J. Padilla, "Perfect metamaterial absorber," *Phys. Rev. Lett.*, Vol. 100, 207402, 2008.

10. Hu, T., N. I. Landy, C. M. Bingham, X. Zhang, R. D. Averitt, and W. J. Padilla, "A metamaterial absorber for the terahertz regime: Design, fabrication, and characterization," *Opt. Express*, Vol. 16, 7181–7188, 2008.

11. Hu, T., C. M. Bingham, D. Pilon, K. Fan, A. C. Strikwerda, D. Shrekenhamer, W. J. Padilla, X. Zhang, and R. D. Averitt, "A dual band terahertz metamaterial absorber," *J. Phys. D: Appl. Phys.*, Vol. 432, 25102, 2010.

12. He, X. J., Y. M. Wang, and T. L. Gui, "Dual-band terahertz metamaterial absorber with polarization insensitivity and wide incident angle," *Progress in Electromagnetics Research,* Vol. 115, 381–397, 2011.

13. Kuznetsov, S. A., A. G. Paulish, A. V. Gelfand, P. A. Lazorskiy, and V. N. Fedorinin, "Matrix structure of metamaterial absorbers for multispectral terahertz imaging," *Progress In Electromagnetics Research,* Vol. 122, 93–103, 2012.

14. Zhang, N., P. Zhou, D. Cheng, X. Weng, J. Xiao, and J. Deng, "Dual-band absorption of mid-infrared metamaterial absorber based on distinct dielectric spacing layers," *Opt. Lett.*, Vol. 38, No. 7, 1125–1127, 2013.

15. Lee, H. M. and H. Lee, "A metamaterial based microwave absorber composed of coplanar electric-field-coupled resonator and wire array," *Progress In Electromagnetics Research C,* Vol. 34, 111–121, 2013.

16. Cheng, Y. Z., H. L. Yang, Z. Cheng, and B. X. Xiao, "A planar polarization-insensitive metamaterial absorber," *Photonics and Nanostructures: Fundamentals and Applications,* Vol. 9, 8–14, 2011.

17. Zhu, B., Z. Wang, C. Huang, Y. Feng, J. Zhao, and T. Jiang, "Polarization insensitive metamaterial absorber with wide incident angle," *Progress In Electromagnetics Research*, Vol. 101, 231–239, 2010.

18. Cheng, Y. Z., Y. Nie, R. Z. Gong, and H. L. Yang, "Multi-band metamaterial absorber using cave-cross resonator," *Eur. Phys. J. Appl. Phys.*, Vol. 56, 31301, 2011.

19. Kollatou, T. M., A. I. Dimitriadis, S. D. Assimonis, N. V. Kantartzis, and C. S. Antonopoulos, "A family of ultra-thin, polarization-insensitive, multi-band, highly absorbing metamaterial structures," *Progress In Electromagnetics Research,* Vol. 136, 579–594, 2013.

20. Huang, L. and H. Chen, "Multi-band and polarization insensitive metamaterial absorber," *Progress In Electromagnetics Research,* Vol. 113, 103–110, 2011.

21. Nornikman, H., B. H. Ahmad, M. Z. A. Abdul Aziz, M. F. B. A. Malek, H. Imran, and A. R. Othman, "Study and simulation of an edge couple split ring resonator (EC-SRR) on truncated pyramidal microwave absorber," *Progress In Electromagnetics Research*, Vol. 127, 319–334, 2012.

22. Zhang, F., L. Yang, Y. Jin, and S. He, "Turn a highly-reflective metal into an omnidirectional broadband absorber by coating a purely-dielectric thin layer of grating," *Progress In Electromagnetics Research*, Vol. 134, 95–109, 2013.

23. Tuong, P. V., V. D. Lam, J. W. Park, E. H. Choi, S. A. Nikitov, and Y. P. Lee, "Perfect-absorber metamaterial based on flower-shaped structure," *Photonics and Nanostructures: Fundamentals and Applications*, Vol. 11, 89–94, 2013.